# Blueing, Bleaching, and Blinking of Single CdSe/ZnS Quantum Dots

Wilfried G. J. H. M. van Sark,*[a] Patrick L. T. M. Frederix,[a, b] Ageeth A. Bol,[c] Hans C. Gerritsen,[a] and Andries Meijerink[c]

*Room temperature time-resolved luminescence measurements on single CdSe/ZnS quantum dots (QDs) are presented. Luminescence spectra were recorded over time periods of up to 30 min with a time resolution down to 6 ms. A clear 30 – 40 nm blue shift in the emission wavelength is observed for QDs in ambient air, before the luminescence stops after about 2 – 3 min due to photobleaching. The blue shift is absent in a nitrogen atmosphere and photobleaching occurs after much longer times, 10 – 15 min. These observations are explained by photoinduced oxidation. During illumination in the presence of oxygen the surface of CdSe is oxidized, which effectively results in shrinkage of the CdSe core diameter by almost 1 nm and, consequently, in a blue shift. This also influences the blinking behavior. The faster fading of the luminescence in air suggests that photoinduced oxidation results in the formation of nonradiative recombination centers at the CdSe/$CdSeO_x$ interface. In a nitrogen atmosphere photoinduced oxidation is prevented by the absence of oxygen. A surprising observation is a higher initial light output for CdSe/ZnS QDs in air. We explain this higher light output by a fast reduction of the lifetime of the long-lived defect states of CdSe/ZnS QDs by oxygen.*

**KEYWORDS:**

optical properties · photoinduced oxidation · photophysics · quantum dots · spectral imaging

Nanometer-sized semiconductor quantum dots (QDs) have received much attention over the past decades as a result of their size-dependent properties.[1–4] Due to the confinement of electrons and holes in the nanocrystallites the energy level scheme resembles that of an atom, with many discrete energy levels. The separation between energy levels increases as the particle size decreases. Moreover, the change in the electronic structure as a function of particle size is evident from the variation of their emission wavelength.[2, 5–7] High quantum efficiencies can be obtained by capping QDs with a passivation layer. Capping of CdSe QDs with a few monolayers of ZnS increases the quantum efficiency considerably to values exceeding 50 %.[8, 9]

The tunability of the optical properties of QDs through changing their size also makes them difficult to study. A prerequisite for the study of QDs is the ability to produce them with a narrow size distribution (< 5 %). Variations of size and shape within ensemble samples result in extensive inhomogeneous broadening of absorption and emission spectra. Measuring spectra of single QDs can circumvent these effects. Since the measurement of *single* quantum dot emission spectra was reported,[10–12] the study of the luminescence of single semiconductor quantum dots has revealed many interesting properties that cannot be observed for an ensemble of many quantum dots. Phenomena of fundamental interest like spectral diffusion and blinking ("on"/"off" behavior[13, 14]) are also important for potential applications of single quantum dots as luminescent labels in biological systems.[9, 15–18]

Most studies on spectral diffusion have been performed at cryogenic temperatures. Random spectral diffusion at these low temperatures has been related to ionization of quantum dots due to Auger processes.[11, 13, 14, 19–23] As a result of the ionization and subsequent recombination processes, the charge distribution around the dot changes, resulting in a spectral (Stark) shift of the emission.[23–25] A clear relation between blinking (explained by photoionization) and the occurrence of a spectral jump has been established. At room temperature, less information is available on spectral diffusion of single QD luminescence. A nonrandom blue shift of about 10 – 15 nm has been reported,[11, 26] which was attributed to photooxidation of the CdSe quantum dot. In a recent study we have observed an irreversible blue shift of up to 40 nm.[27] In this paper, we further report on a time-resolved study of emission spectra of single CdSe/ZnS

[a] *Dr. W. G. J. H. M. van Sark, Dr. P. L. T. M. Frederix,[+] Prof. Dr. H. C. Gerritsen*
*Department of Molecular Biophysics*
*Debye Institute*
*Utrecht University*
*P.O. Box 80000, 3508 TA Utrecht (The Netherlands)*
*Fax: (+31) 30-253-2706*
*E-mail: W.G.J.H.M.vanSark@phys.uu.nl*

[b] *Dr. P. L. T. M. Frederix[+]*
*Department of Medical Physiology*
*Faculty of Medicine*
*Utrecht University*
*P.O. Box 80030, 3508 TA Utrecht (The Netherlands)*

[c] *Dr. A. A. Bol,[++] Prof. Dr. A. Meijerink*
*Department of Physics and Chemistry of Condensed Matter*
*Debye Institute*
*Utrecht University*
*P.O. Box 80000, 3508 TA Utrecht (The Netherlands)*

[+] *Present address:*
*M. E. Müller Institute, Biocenter*
*University of Basel*
*Klingelbergstrasse 70, 4056 Basel (Switzerland)*

[++] *Present address:*
*Philips Research Laboratories*
*Prof. Holstlaan 4, 5656 AA Eindhoven (The Netherlands)*

quantum dots. Results are presented on spectral diffusion (blueing), the disappearance of the emission (bleaching), and "on"/"off" behavior (blinking). Data are taken over time periods up to 30 min with a time resolution down to 6 ms. We have studied two types of CdSe quantum dots, differing in the thickness of the ZnS shell. Since the photophysical properties of QDs depend on their local environment, as recently reported,[18, 26, 28] we have also studied the QDs in air as well as in ambient nitrogen.

## QD Size, Spectra, and Lifetimes

From HR-TEM images, the sizes of the crystalline CdSe/ZnS nanoparticles were determined. In Figure 1 a histogram of the size distribution of batch **1** (CdSe with a shell of four ZnS monolayers) is shown, where we analyzed 147 QDs. Due to poor

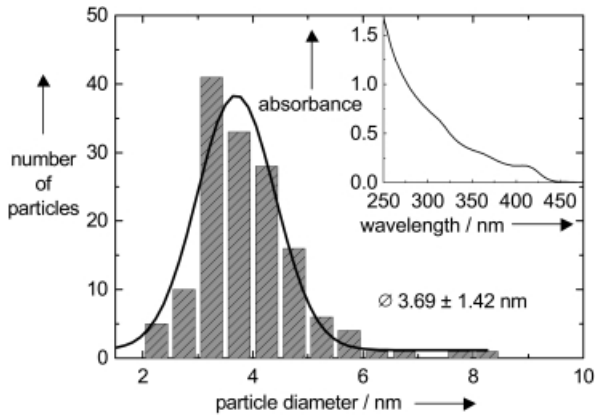


***Figure 1.*** *Histogram of the particle size distribution of nanocrystalline CdSe QDs overgrown with four monolayers of ZnS (batch **1**) as determined from HR-TEM images. Inset: The UV-Vis absorption spectrum.*

contrast in the pictures it was not possible to distinguish between the CdSe core and the ZnS shell. As can be seen in Figure 1 the width of the size distribution of batch **1** is quite large (≈50%). The average particle diameter of the CdSe/ZnS core shell QDs is 3.7 ± 1.4 nm. Similar results were obtained for batch **2** (CdSe with a shell of seven ZnS monolayers).

A typical absorption spectrum of a sample of CdSe/ZnS quantum dots is shown as an insert in Figure 1. Due to quantum size effects the absorption spectra of the CdSe/ZnS nanoparticles has shifted to the blue compared to the absorption spectrum of bulk CdSe (onset around 730 nm[29]). The structure in the absorption band is a result of the formation of discrete energy levels caused by quantum size effects. This structure is still visible, despite the large width of the size distribution. The polydispersity of the sample is also reflected in the emission spectrum: It shows a broad band centered on 650 nm with a large full width at half maximum (FWHM).[30] The luminescence intensity increases strongly upon the growth of the ZnS shell around the CdSe core. The luminescence quantum efficiency of the nanocrystalline CdSe/ZnS is determined to be typically 30%, whereas the uncapped CdSe has a quantum efficiency of 5%.

To confirm the excitonic nature of the QD fluorescence so as to exclude trap emission, lifetime imaging measurements were performed with the eight-gate lifetime aquisition module (Limo) and the two-photon excitation (TPE) microscope. A typical result is shown in Figure 2, where the intensity per time gate is plotted

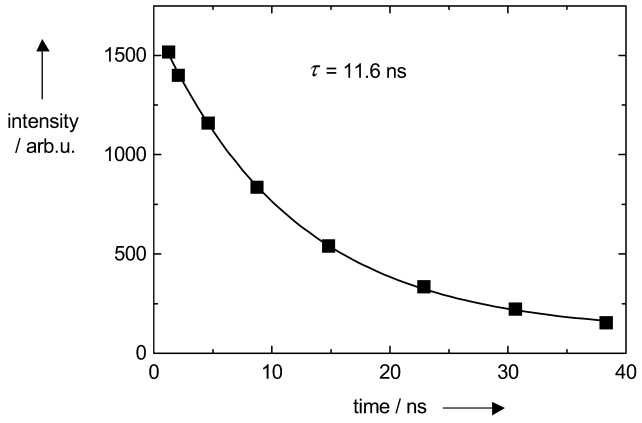


***Figure 2.*** *Fluorescence intensity per time gate as a function of time after the excitation pulse. The fluorescence lifetime τ determined from a monoexponential fit is 11.6 ± 0.3 ns.*

as a function of time after the laser pulse. A monoexponential fit yields a lifetime $\tau$ of 11.6 ± 0.3 ns. Although a double exponential fit yields a slightly better $\chi^2$, with lifetimes of 9 and 16 ns, in the following we used only monoexponential fits. Recently, Schlegel et al. have found the fluorescence lifetime to fluctuate during measurements, which is reflected as a wide distribution of lifetimes.[31] A long lifetime is correlated with high fluorescence intensity. For our QDs we determined lifetimes between 8 and 30 ns. Interestingly, the fitted lifetime depends on the excitation intensity. Figure 3 a shows the lifetime as a function of excitation intensity relative to 500 kW cm$^{-2}$, measured by using neutral density filters. For the three QDs shown, differing in their emission wavelength, the lifetime seems to increase with decreasing excitation intensity. This may be explained by the formation of biexcitons at high excitation that have a shorter lifetime than excitons, as reported by Woggon et al.[32] We are currently setting up single QD lifetime measurements in order to further substantiate these findings. The apparent decrease of lifetime with QD size, as can be inferred from the lower lifetimes for the QDs with higher emission wavelength, is due to differences in quantum efficiency rather than size. Figure 3 b shows the emission intensity to be dependent on the square of the excitation intensity, which proves that two-photon excitation occurs. Similar graphs were reported by Lakowicz et al. in a TPE study of CdS nanoparticles. The relative ease with which TPE can be performed on QDs is due to the high cross-sections. Lakowicz et al.[33] report a TPE cross section of $10^{-48}$ cm$^4$ s photon$^{-1}$ at 700 nm, which is much larger than the one for fluorescein at 700 nm.[34, 35] Blanton et al.[10] calculated cross-sections as large as $10^{-46}$ cm$^4$ s photon$^{-1}$ at 800 nm.

Individual QDs and their emission spectra could easily be resolved by using fast spectral imaging with the confocal laser-

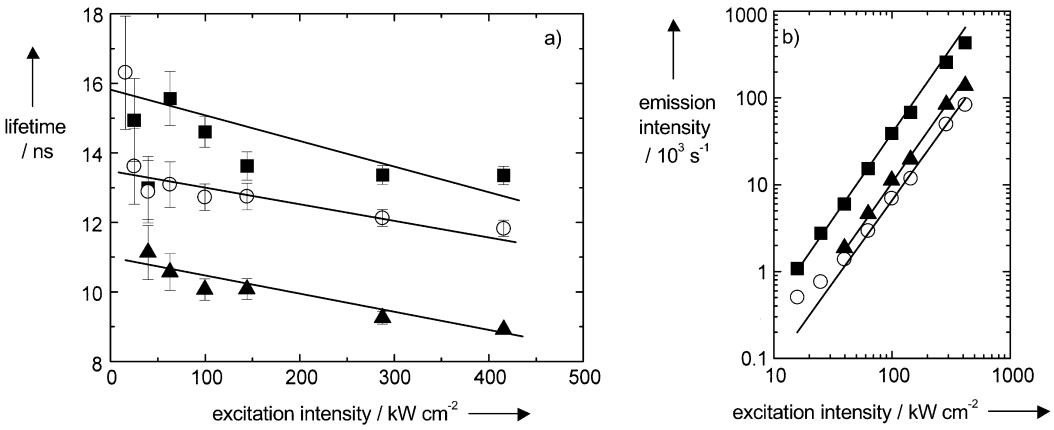


***Figure 3.*** *a) Fluorescence lifetime as a function of excitation intensity for three QDs with emission wavelength $\lambda_{em}$ of 555 (■), 585 (○), and 607 nm (▲). The lines are drawn as a guide to the eye. b) Two-photon induced emission intensity as a function of excitation intensity. The slopes are 1.9 ± 0.1, 2.0 ± 0.1, and 2.0 ± 0.1 for the QDs emitting at $\lambda_{em}$ 555, 585, and 607 nm (symbols as above), respectively.*

scanning microscope (CLSM)/spectrograph set-up. In Figure 4 the spectra of a few of these QDs of batch **1** are shown, with emission wavelengths of 538, 562, 601, 619, and 640 nm, and

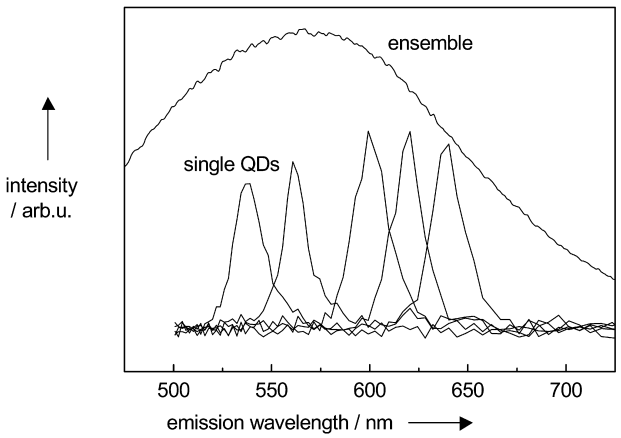


***Figure 4.*** *Fluorescence emission spectra of several single QDs recorded with the CLSM/spectrograph set-up, compared to the spectrum of an ensemble of QDs. The emission wavelengths $\lambda_{em}$ of the single QDs are 538, 562, 601, 619, and 640 nm ($\lambda_{ex}$ = 468 nm).*

narrow FWHMs between 13 and 18 nm. The corresponding diameters are calculated to be 3.5, 4.1, 5.3, 6.1, and 7.1 nm, respectively.[6] The integrated emission spectrum over many imaged areas, "ensemble", is shown for comparison. It is clear that, due to the large size distribution the emission spectrum of an ensemble of CdSe/ZnS quantum dots is substantially broadened compared to the emission spectrum of a single quantum dot. The value of the emission linewidth of single quantum dots is in agreement with the homogeneous broadening at room temperature by phonon dephasing processes.[36]

## Blueing

We have measured the luminescence spectra of a large number (41) of individual CdSe/ZnS quantum dots in different atmospheres. Clear differences are observed between these time-resolved emission spectra, even for quantum dots of the same batch in the same atmosphere. Results are summarized in Table 1. In Figure 5 a a typical spectrally resolved time trace (duration 80 s) is presented of a CdSe/ZnS QD of batch **1** in *air*. Initially this QD emits at 585 nm (for about 20 s), and then the emission wavelength starts to shift to the blue. After a shift of about 40 nm the emission of the QD is fully photobleached. Also, blinking can readily be observed. Figure 5 b shows spectra of the QD collected (6 ms integration) at different times. The two spectra recorded at the later times, such as at 38.8 and 50.6 s, are clearly blue shifted (by 12 and 32 nm, respectively) with respect to the initial wavelength of 585 nm. The positions of the maxima, the integrated intensity, and FWHM of the emission bands were determined by fitting the spectra with a Lorentzian.[2] The FWHM of the peaks is about 15 nm and hardly changes with time. The result of fitting the emission maxima is shown in Figure 6 a, where the emission wavelength of a CdSe/ZnS QD from batch **1**

***Table 1.*** *Blue shift, bleaching time, blinking parameters $m_{on}$ and $m_{off}$, and total detected intensity of the luminescence of 41 QDs.*[a]

| Batch | Ambient | Number of QDs | Blue shift [nm] | Bleaching time [s] | Blinking parameter $m_{on}$ | Blinking parameter $m_{off}$ | Total detected intensity $\times 10^6$ photons |
|---|---|---|---|---|---|---|---|
| **1** (4 ML ZnS) | Nitrogen | 4 | 4 ± 5 | 775 ± 524 | 2.04 ± 0.23 | 1.23 ± 0.09 | 0.66 ± 0.39 |
| | Air | 12 | 29 ± 17 | 140 ± 184 | 1.58 ± 0.24 | 1.44 ± 0.16 | 0.34 ± 0.32 |
| **2** (7 ML ZnS) | Nitrogen | 9 | 2 ± 3 | 500 ± 333 | 2.33 ± 0.42 | 1.17 ± 0.12 | 1.4 ± 0.8 |
| | Air | 16 | 29 ± 10 | 214 ± 293 | 1.78 ± 0.47 | 1.33 ± 0.19 | 0.84 ± 0.74 |

[a] Errors are the standard deviations of the distribution.

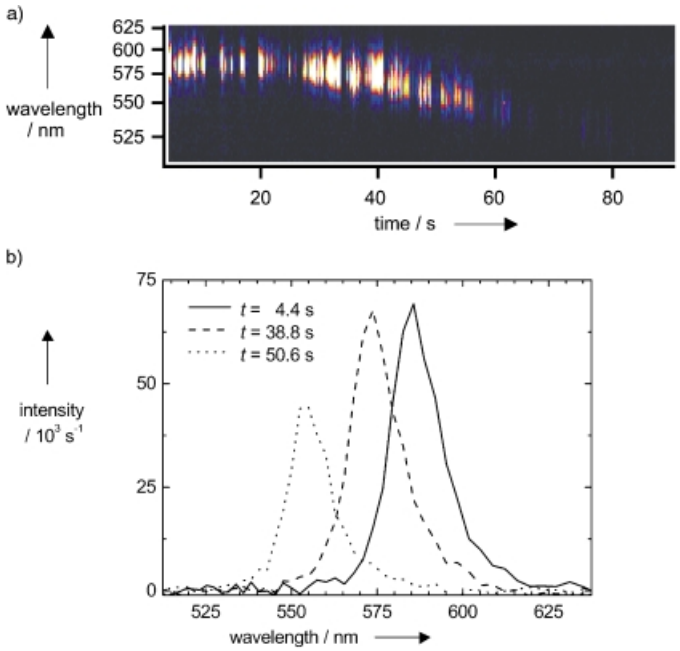


***Figure 5.*** *a) Spectrally resolved time trace of a batch **1** CdSe/ZnS QD in ambient air present in the detection volume of the CLSM/spectrograph set-up. Note that the intensity is a stretched false color representation. b) Emission spectra at different illumination times.*

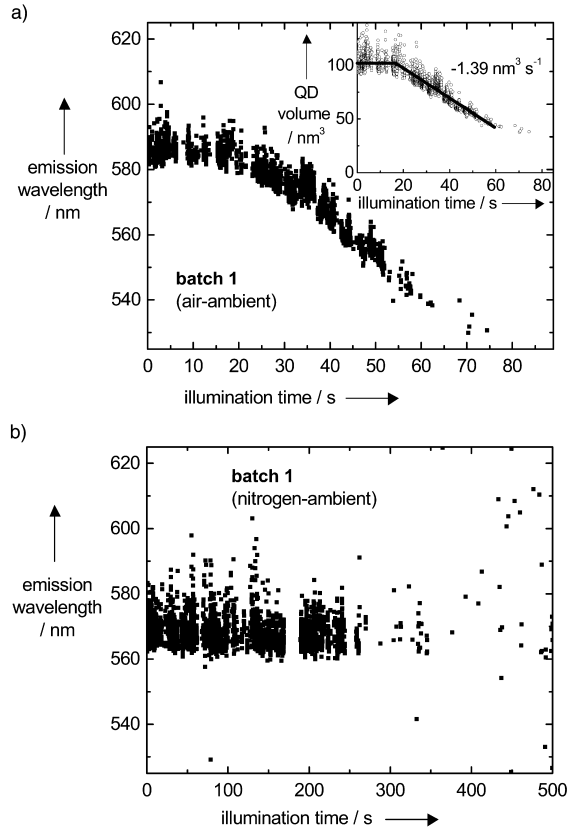


***Figure 6.*** *a) Fitted emission wavelength as a function of time for the CdSe/ZnS QD of Figure 5 (batch **1**, air). Inset: The calculated QD volume as a function of time. Note that the oxidation sets in at 20 s with a constant rate of $-1.39\ nm^3\ s^{-1}$. b) Emission wavelength as a function of time for a batch **1** CdSe/ZnS QD in nitrogen. Note the much larger time scale compared to (a).*

in air is depicted as a function of time. Other quantum dots of batch **1** and **2** in air show similar results. The average blue shift amounted to $29 \pm 10$ and $29 \pm 17$ nm, respectively, before the luminescence disappears; see Table 1. In some cases an initial fast blue shift is observed, while for most QDs a behavior similar to that depicted in Figure 6a is observed.[37] For QDs of batch **1**, the luminescence intensity decreases in time and no luminescence is observed after, on average, 2.5 min (Table 1). There are large differences between quenching times for individual dots, in agreement with previously reported results.[11, 27] The time scales for the blue shift and the photobleaching for QDs from batch **2** are observed to be significantly longer (bleaching occurs on average after 3.5 min). This is obviously due to the increased thickness of the passivating ZnS.

The time-evolution of the fitted emission wavelength for a single CdSe/ZnS QD of batch **1** in a nitrogen atmosphere is depicted in Figure 6b. Clearly, a blue shift is absent. A reversible spectral variation of 10 nm is observed around a central emission wavelength of about 570 nm. This is in agreement with previous measurements, which show that over longer time periods random spectral diffusion can result in shifts of up to 10 nm.[38, 39] Contrary to the situation in *air*, there is only random spectral diffusion in time and no shift to shorter wavelengths is observed. Photobleaching of the QDs in nitrogen sets in after much longer times, around 10 min on average for both batches (see Table 1).

The observed differences between the time evolution of the emission spectra of single quantum dots in air and in nitrogen provide convincing evidence that the observed blue shift of the emission in air is due to photooxidation of CdSe. From the amount of blue shift and the relation between the bandgap and diameter of CdSe particles[2, 5–7] we have calculated that the effective CdSe core diameter decreases from about 5 to about 4 nm before the QD is completely bleached. The inset in Figure 6a shows the calculated QD volume as a function of time. For the calculation we have used the data on the relation between emission wavelength and QD radius for CdSe as reported by Mikulec et al.[5] It is clear from the plateau in Figure 6a that oxidation starts after about 20 s and the volume decrease per unit of time is constant at $-1.39\ nm^3\ s^{-1}$. As the oxidation rate measures the mass decrease rate of the QD, a constant volume decrease rate implies that the oxidation rate is constant.

A change in particle diameter of 1 nm corresponds to photooxidation of almost two layers of CdSe from the surface.[11] We have observed blueing even under low illumination levels ($\sim 0.5\ W\ cm^{-2}$), by using the Xe lamp in the spectrofluorometer as irradiation source. Blueing then occurs overnight. Similar results on surface oxidation of CdSe nanoparticles have been reported.[40] The main oxidation product was suggested to be $SeO_2$. Photooxidation is well understood for CdS nanocrystals.[41–43] Upon illumination in solution, CdS nanocrystals are photooxidized to $Cd^{2+}$ and $SO_4^{2-}$. The difficulty of obtaining photostable CdTe nanocrystals has also been attributed to oxidation.[44] For photooxidation of CdSe, evidence for the formation of $CdSeO_x$ ($x = 2$[6, 40] and 3[41]) has been found. In the

present experiments the nature of the photooxidation product has not been analyzed. For photooxidation of the CdSe core to take place, oxygen has to diffuse through the passivating ZnS layer covering the CdSe nanocrystals.

The occurrence of photooxidation indicates that the ZnS layer is not a closed epitaxial layer but rather a layer with grain boundaries, presumably at places where ZnS islands, which started growing at different locations on CdSe, meet. At these boundaries oxygen can diffuse to the CdSe core inside the ZnS shell. With a thicker shell (batch **2**) the oxidation rate is reduced (not shown) due to the slower diffusion of oxygen to the CdSe core through a thicker ZnS shell. Alternatively, photoinduced oxidation of the ZnS shell would break down the ZnS lattice, resulting in a more porous structure. Degradation of the shell would thus create an increasing interface of the CdSe core to the surrounding air. A fast oxidation of the CdSe core is delayed until the shell has degraded. Also, the oxidation products of the CdSe core could rupture the ZnS shell, and accessibility of oxygen is enhanced as well.

The nature of these oxidation paths is different. Upon excitation of the QD the electron most likely is expelled from the core,[6, 45] and the oxidation is expected to occur from a positively charged QD. If the oxidation starts directly at the interface of the CdSe core and the ZnS shell, the expelled electron from the core is expected to be scavenged by an oxygen molecule that has diffused through the ZnS cap. If the oxidation starts at the outer layer of the ZnS shell, the electron that has left the QD core supposedly reacts with an adsorbed oxygen molecule to form $O_2^-$. A similar oxidation would then follow as was reported for ZnS QDs.[41]

## Bleaching

As presented above, QDs of batch **1** in air are bleached after typically 2.5 min, while large differences between quenching times for individual dots exist (see also the error margins in Table 1). In addition, a gradual decrease of the emission count rate in time was observed for QDs before they were totally bleached. The amount of this gradual decrease typically correlates well with the amount of blue shift. Due to the increased thickness of the passivating ZnS layer for QDs from batch **2**, the time scales for the photobleaching (and the blue shift) in air are longer: Bleaching occurs on average after 3.5 min.

The time periods for which the dots show emission (until photobleaching occurs) are significantly longer for the QDs in nitrogen than in air (about 10 min on average for both batches). In nitrogen the QDs from batch **2** bleach somewhat faster than the QDs from batch **1**, see Table 1. This may be related to a larger number of defects in the ZnS capping layer with a larger capping thickness. For a ZnS capping thickness exceeding 1.3 monolayers, a decrease in the luminescence quantum yield was observed[6] and attributed to an increased amount of defects. It was suggested that, most likely, the start of the ZnS growth was coherent with the underlying CdSe core but became incoherent at larger ZnS thickness. The lattice mismatch of a ZnS film on a CdSe substrate $f$ is about $+12\,\%$, that is $f = [a_0(\mathrm{CdSe}) - a_0(\mathrm{ZnS})]/a_0(\mathrm{ZnS})$, where $a_0$ is the unstrained lattice constant.[46, 47] The ZnS shell will be highly strained in tension. The curved surface of the CdSe core will even result in a larger tensional strain. As a result of the large strain caused by the lattice mismatch, it is very likely that dislocations are formed as well as low-angle grain boundaries.

The intensity decrease for the QDs in air can be partly explained by the size reduction of the QD core as a result of the photooxidation. For QDs smaller than 5 nm in diameter it has been reported that the absorption cross-section decreases with decreasing core size.[2] This intensity decrease is indeed observed for the QDs in air during the blue-shift.[37] However, the reduction in the QD core size alone cannot explain the reduction of emission intensity to zero. Also, an intensity decrease is observed for the QDs in nitrogen, where a blue-shift is absent and hence their size is not reduced. It is therefore more likely that the intensity decrease and bleaching are caused by the formation of lattice defects in the QDs, thereby creating additional nonradiative recombination pathways (quenching states). A number of these defects might be annihilated again, which explains part of the intensity fluctuations.[38] Defects that are not annihilated, those that are permanent, eventually result in a complete quenching of the luminescence. The precise role of oxygen in this is not clear.

For the QDs in air the quenching states are expected to be formed at the CdSe/$CdSeO_x$ interface. The formation of surface quenching states causes a decrease of the number of photons emitted. In the single QD emission spectra a gradual and simultaneous decrease in light output is indeed observed as the emission shifts to shorter wavelengths. Finally, the luminescence disappears and the QD has bleached. The occurrence of photooxidation for QDs can explain the shorter bleaching times observed for QDs in air. In a nitrogen atmosphere photobleaching also occurs, albeit after much longer times. In view of the high laser power (20 kW cm$^{-2}$) photobleaching is not unexpected; few materials are stable against photodegradation under the presently used laser power. The nature of the photoinduced quenching states is not clear. The efficiency of the photoinduced formation of quenching states in nitrogen is much lower than for photooxidation observed in air. Possibly, a high-energy biexciton state in a single dot has enough energy to rearrange or break bonds at the CdSe/ZnS interface, which gives rise to additional nonradiative recombination channels. From the absence of a blue shift for QDs in nitrogen it can be concluded that the defects do not cause a significant reduction in the QD core volume. The longer time scale for quenching in *nitrogen* shows that the efficiency of photoinduced formation of quenching states in nitrogen is much lower than that of photooxidation.

## Blinking

The blinking behavior of the ZnS-coated CdSe QDs is evident from Figure 5, and is shown more clearly in Figure 7 for both ambient nitrogen and air. It was quantified by determining the "off" and "on" time distributions from the spectral time-traces. The emission intensity was used a means to distinguish between "on" and "off" state. A threshold set just above the background was carefully determined to discriminate between the states.

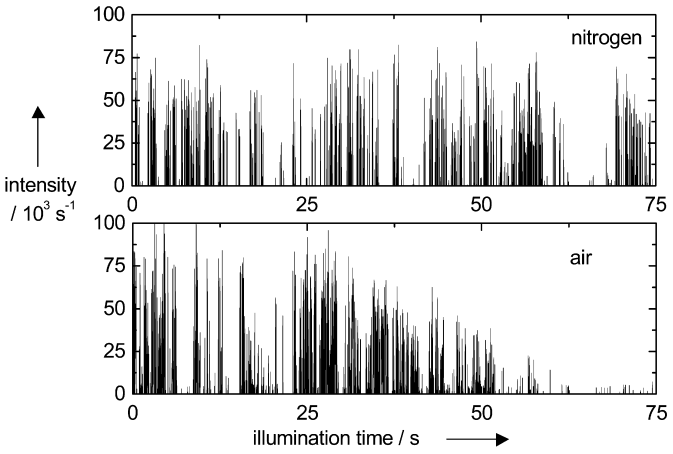


***Figure 7.*** *Emission intensity time traces of QDs in nitrogen and air followed for 75 s. Data are extracted from the spectral time traces as depicted in Figures 6a and 6b.*

Figure 8 shows the "off" and "on" time distributions for single QDs of batch **2** in air and in nitrogen. We have used the procedure reported by Kuno et al.[13] First, a raw histogram of "off" times (or "on" times) is determined from a time-trace as shown in Figure 7. A continuous probability density then is generated from the histogram by weighing with the average time between nearest-neighbor events.

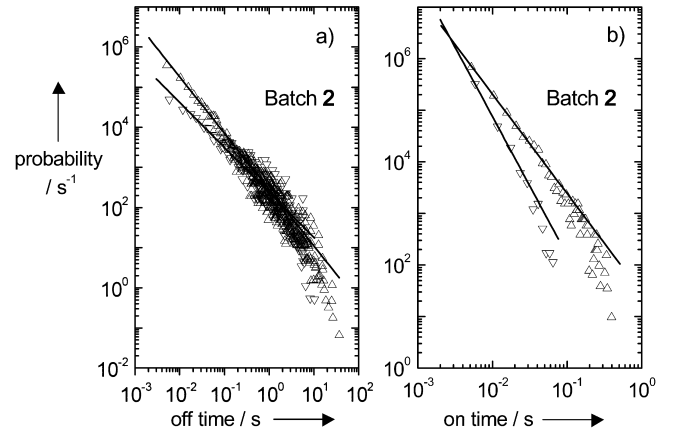


***Figure 8.*** *a) "Off" and b) "on" time distributions for batch **2** QDs in air (△) and nitrogen (▽). The distributions of these particular QDs can be fitted using a power law with coefficients* $m_{off} = 1.40$ *and* $m_{on} = 1.93$ *(in air) and* $m_{off} = 1.12$ *and* $m_{on} = 2.69$ *(in nitrogen). Note the differences in probability and time scales.*

Analysis of the distribution of "off" time intervals for all QDs shows that the probability density of "off" time intervals can be described by an inverse power law, in accordance with Kuno et al.[13, 14] Fitting the data in Figure 8a to a power law distribution yields $m_{off} = 1.40$ (air) and $m_{off} = 1.12$ (nitrogen) for this particular QD. For the two batches and the two atmospheres, the blinking coefficients $m_{off}$ are summarized in Table 1. For our 41 QDs we find an average value of $m_{off} = 1.4 \pm 0.2$, in correspondence to earlier reported values.[13] In addition, a power law distribution of the "on" time intervals is seen in Figure 8b, namely $P(t_{on}) \propto 1/(t_{on}^{m_{on}})$. Fitting the data to this power law distribution yields $m_{on} = 1.93$ (air) and $m_{on} = 2.69$ (nitrogen). In Table 1 the blinking coefficients $m_{on}$ for all dots are summarized.

The study by Kuno et al.[13, 14] on blinking behavior provides evidence for an inverse power law behavior of both the "off" and "on" time intervals. They observed excellent agreement between the experimentally observed "off" time distribution and an inverse power-law description over nine decades in probability density and five decades in time, with $m_{off} = 1.6 \pm 0.2$.[13, 14] For the "on" time distribution they report seven decades in probability density and five decades in time, with $m_{on} = 1.9 \pm 0.1$.[14] In contrast, in a recent study Shimizu et al.[48] reported $m_{off} = m_{on} = 1.5$ and, in addition, showed that $m_{off}$ is independent of temperature in the range from 10 K to room temperature. Note that our data for QDs in air (see Table 1) closely resemble those reported by Kuno et al.[13] This is not surprising, since their data were taken in air as well.[14] The most probable explanation for the inverse power law behavior of the "off" state is the existence of multiple ionization states and consequently a distribution of recombination rates. Since the process that leads to the "off" state is assigned to photoionization (by an Auger process) of the QD, the "off" time intervals are related to recombination of the ejected charge carrier with the ionized dot. Therefore, a difference in blinking behavior in air and in nitrogen is expected as the shrinking of the CdSe core and the formation of a $CdSeO_x$ at the interface is likely to influence the tunneling rate for recombination of an ejected charge carrier and an ionized dot. The data shown in Table 1 indicate that somewhat lower values of $m_{off}$ are obtained for QDs in nitrogen in comparison to air, namely average "off" times in nitrogen are somewhat longer. In air, preliminary data suggest that the "off" times are longer in the blue-shift phase. From a recent study by Koberling et al.[28] a small difference in "off" time distribution can be inferred between blinking in argon and in oxygen, similar to that presented here.

In contrast, a large difference in the "on" time distribution is observed by Koberling et al.,[28] as represented by them as a difference in mean "on" times. In argon the mean "on" time, equivalently the probability of longer "on" times, is larger than in the case of oxygen. This was explained by an oxygen-induced reduction of fluorescence lifetime. Our data show that in nitrogen the probability of long "on" times is smaller than in the case of air. It will be discussed below that for our experimental conditions, namely high excitation intensity, it is likely that oxygen quenches the defect luminescence. As a result, the apparent fluorescent lifetime is enhanced. Note that the difference in excitation intensity between the study by Koberling et al.[28] and ours is nearly three orders of magnitude, 45 (Koberling et al.[28]) versus 20 kW cm$^{-2}$. At present, further research is in progress to study in detail differences in the blinking of QDs in different ambients.

In order to explain the inverse power-law behavior of the "on" time distribution, Kuno et al.[14] proposed that electron tunneling events are involved, which photoionize a QD. Tunneling must occur to sites several nanometers outside the QD in order to account for the large dynamic range in "off" and "on" time

distributions. Therefore, a difference in the local environment (and fluctuations therein) of the QD is expected to be reflected in the blinking coefficients $m_{off}$ and $m_{on}$. The results shown in Table 1 support this.

## Total Photon Yield

The potential application of single quantum dots as luminescent labels (such as in biological systems) is based on the high stability in combination with a relative narrow emission band and a large Stokes' shift.[9, 15] The total number of photons emitted by a single QD until bleaching occurs, denoted also as the turnover number, quantifies the stability of a moiety. For single dye molecules (for example for Rhodamine[49–51]) the highest number of photons emitted before bleaching is around $10^6$ at room temperature. Based on an overall efficiency of about 5% for our detection system (counts one of every twenty emitted photons), the number of photons emitted by a single QD before bleaching occurs is typically $2 \times 10^7$, exceeding $10^8$ for the more robust quantum dots. Messin et al. report a value of $3 \times 10^7$ photons.[52] Interestingly, a value of as high as $10^9$ has been reported recently.[14] These numbers are more than an order of magnitude higher than for single dye molecules, which reflects the higher stability of inorganic chromophores such as these semiconductor QDs.[15, 17]

Surprisingly, the total number of photons emitted before bleaching occurs is not much less for QDs in air than for in nitrogen (see Table 1). The lower photostability of QDs in air is compensated for by a higher initial photon count in air. The initial emission intensity is about twice as high for QDs in air (about 3000 counts, versus 1500 counts in nitrogen during the 6 ms integration period for the brightest QDs). A possible explanation for the higher initial light output in air is quenching of QD defect luminescence by oxygen. It is well known that in addition to the fast (nanosecond) exciton emission, also relatively long-lived (microsecond) defect emission can occur in QDs.[41, 53] Due to the long lifetime, the fast photon absorption and emission process is interrupted, until the long-lived excited state has returned (via radiative or nonradiative relaxation) to the ground state. If oxygen can quench the defect luminescence, a higher exciton emission yield is expected by reduction of the time spent in the dark state. It has been established that oxygen can quench the defect-related emission for other II–VI semiconductors like CdS and ZnS.[41, 53] Supposing that the same occurs for CdSe QDs, as inferred from results reported by Cordero et al.,[26] this can explain the higher initial light output observed for CdSe QDs in air. The presently applied excitation power ($20\,kW\,cm^{-2}$) yields initial intensities of 1000–3000 counts in 6 ms. Assuming a 5% collection efficiency, this corresponds to time intervals of 100–300 ns between emission of photons. In this situation relaxation to a trap state with a microsecond lifetime will reduce the number of photons emitted and a fast return to the ground state by nonradiative relaxation enhances the photon output. A similar situation has been reported for organic dye molecules where higher fluorescence light yields were measured as a result of shortening of the triplet-state lifetime by oxygen.[54] In addition, it has been reported that most probably the adsorption of water molecules rather than oxygen is responsible for the strong influence on fluorescence intensity.[26, 55] We are presently pursuing time-resolved measurement of excitons and defect lifetimes of QDs in various ambients in order to elucidate the role of oxygen.

## Conclusion

We have presented time-resolved luminescence measurements on single CdSe/ZnS core-shell QDs. A clear blue shift in the emission wavelength of about 30 nm on average is observed in ambient air. In contrast, this shift is not observed for QDs in nitrogen. Moreover, the bleaching time, blinking behavior, and initial emission intensity of single QDs are influenced by the presence of oxygen. The results are discussed in relation to photoinduced oxidation of the CdSe crystallites and oxygen-induced quenching of defect states.

## Experimental Section

The ZnS-capped CdSe nanoparticles were synthesized by using the wet chemical tri-*n*-octylphosphine/tri-*n*-octylphosphine oxide (TOP/TOPO) method similar to that described by Hines and Guyot-Sionnest.[8, 56] Two batches of overcoated dots were synthesized: For batch **1** about 4 monolayers of ZnS were grown over the CdSe core, while for batch **2** the thickness amounted to about 7 monolayers. The number of monolayers is based on the amounts of precursors used in the synthesis. TOP, TOPO, anhydrous methanol, and anhydrous chloroform (Aldrich); diethylzinc (DEZn) and dimethylcadmium (DMCd) (Strem Chemicals); bis(trimethyl)silylsulphide ($(TMS)_2S$) (Fluka); and Se powder (Chempur) were purchased.

The synthesis was performed in a glovebox filled with dry $N_2$. Stock solutions of Cd/TOP, Zn/TOP, Se/TOP, and S/TOP were prepared by dissolving DMCd, DEZn, Se, and $(TMS)_2S$ in TOP [1.6 g (11 mmol) in 15.5 mL, 1.23 g (10 mmol) in 9.0 mL, 1.3 g (16 mmol) in 16.0 mL, and 2.0 mL (10 mmol) in 8.0 mL, respectively]. The (Cd,Se)/TOP [(Zn,S)/TOP] stock solution, freshly prepared for every synthesis, required dissolving Cd/TOP (0.4 mL) plus Se/TOP (0.4 mL) in TOP (2.0 mL) [S/TOP (1.6 mL) plus Zn/TOP (1.12 mL) in TOP (8.28 mL)]. TOPO (25 g) was heated to 300 °C and maintained there for half an hour. The temperature was then raised to 370 °C, after which the heater was removed. At 360 °C the (Cd,Se)/TOP stock solution (1.4 mL, 0.13 mmol Cd, 0.20 mmol Se) was rapidly injected. A small sample of bare CdSe QDs was isolated for characterization. The reaction mixture was allowed to cool to 300 °C and at this temperature the (Zn,S)/TOP stock solution (5.5 mL, 0.62 mmol Zn, 0.88 mmol S) was added in five portions at approximately 20 s intervals (batch **1**). For batch **2**, a larger amount of (Zn,S)/TOP (13.73 mL) was added in five portions, to yield a thicker ZnS shell. After this injection the reaction mixture was allowed to cool to 100 °C and kept at this temperature for 1 h. The nanocrystals were purified by precipitation with anhydrous methanol. The precipitate was collected by centrifuging (4000 rpm, 5 min) and then washed three times with anhydrous methanol. The nanocrystals were dispersed in doubly distilled chloroform and stored.

Samples were characterized by UV/Vis absorption spectroscopy (Perkin-Elmer double beam Lambda 16 spectrophotometer), HR-TEM (Philips CM300UT-FEG, 300 kV), and emission and excitation spectroscopy (SPEX Fluorolog spectrofluorometer, two double-grating 0.22 m SPEX 1680 monochromators, 450 W Xe lamp, emission detected with a cooled Hamamatsu R928 photomultiplier). The

presented emission spectra have been corrected for the wavelength-dependent sensitivity of the photomultiplier.

The luminescence quantum efficiency of a sample was determined by comparing the integrated emission intensity to that of a reference solution sulforhodamine 101 (Molecular Probes) in EtOH ($\lambda_{ex}$ 586 nm, $\lambda_{em}$ 605 nm, $\varepsilon$ 108000 $cm^{-1}M^{-1}$, luminescence quantum efficiency close to 90%),[57] in which the position of the emission band of the reference was as close as possible to that of the sample. The absorbance at the excitation wavelength is low and similar for both the sample and the reference solution. When necessary the solutions were diluted in order to have an absorbance such that the emission intensity scales linearly with the number of absorbed photons.

For single particle luminescence measurements, small droplets of a strongly diluted QD stock solution were deposited, spread, and dried on cover glass slides. The final density was approximately 0.1 $\mu m^{-2}$. The slides were prepared, mounted, and sealed in a flowchamber in nitrogen. Prior to and during the experiments dry nitrogen or air was flushed through the flowchamber.

Fast spectral imaging of single dots was performed employing a CLSM (Nikon PCM2000). An Ar–Kr CW laser (468 nm, 20 $kW cm^{-2}$) was used for excitation. The emission was collected through a 50 μm pinhole of the CLSM and using a 60 × /1.4 oil immersion objective (Nikon, PlanApo). The two detection channels of the microscope were coupled to the detectors by means of optical fibers. In the configuration applied here, one of the standard detectors (photomultiplier tubes) was replaced by a home-built spectrograph.[37, 58] In the spectrograph the light was dispersed by a prism (SF10 glass, 60 mm equilateral), and detected with a Peltier-cooled, back-illuminated CCD camera (Princeton Instruments, NTE/CCD-1340). The spectral resolution is wavelength-dependent and varied between 1.5 and 5.5 nm (from 500 to 700 nm) in the measurements presented here. The second photomultiplier tube of the CLSM was first used to locate a single QD, employing a 590/60 bandpass filter (Nikon). After positioning the laser beam on a single QD, the emission light is coupled into the spectrograph and the spectra were recorded with a 6 ms dwell time. The luminescence of QDs was followed until the luminescence had been bleached away (1–30 minutes). Data were corrected for the background signal by subtracting the average spectrum from the time interval of the recording where the QD was not emitting. Data were further corrected for the detection sensitivity of the set-up using a calibrated tungsten band lamp. Its temperature and spectrum were recorded and compared to the theoretical spectrum of a blackbody radiator of the same temperature. In order to quantify of the integrated intensity, the peak position, and the peak width the spectra were fitted by a Lorentzian peak function.[2]

Fluorescence lifetime experiments were performed with a home-built TPE microscope set-up.[59, 60] This system is equipped with a mode-locked tunable Ti:sapphire laser (Tsunami, Spectra-Physics), which produces 80 fs pulses at a repetition rate of 82 MHz. A pulse picker (Spectra-Physics) is used to reduce the repetition rate to 8.2 MHz. The excitation light was focused by a 60 × /1.4 oil immersion objective (Nikon, PlanApo) and is scanned over the sample at 256 μs pixel dwell time. The fluorescence light was collected by the same objective, transmitted through a dichroic mirror, and directed towards a home-built fluorescence lifetime acquisition module (Limo).[61] In this eight-channel time-gated detection system a high sensitivity is realized by opening all the gates sequentially after each and every excitation pulse. In this way, effectively the whole decay can be captured without losing any photons. The widths of the gates can be set independently and optimized for the measured lifetimes. Here we used as gate settings 4, 4, 4, 4, 8, 8, 10, and 10 ns, yielding a total width of 52 ns, well below the interpulse distance of 122 ns. The Ti:sapphire laser was tuned to 700 nm. Thorough blocking of excitation light is achieved by means of a series of 660 nm interference short-pass filters. Attenuation was achieved by using neutral density filters (O.D. 0.08 – 1.5).

*We thank Joost van Lingen, Sander Wuister, and Celso de Mello Donegá for help with QD synthesis, Dave van den Heuvel for spectroscopic investigations, and Gwendal Latouche for assistance with the TPE lifetime measurements. Further, we gratefully acknowledge the Netherlands Technology Foundation (STW) and the Netherlands Council for Earth and Life Sciences (ALW) of the Netherlands Organization for Scientific Research (NWO) for financial support.*

[1] A. P. Alivisatos, *J. Phys. Chem.* **1996**, *100*, 13226 – 13239.
[2] S. V. Gaponenko, *Optical Properties of Semiconductor Nanocrystals,* Cambridge University Press, Cambridge, **1998**.
[3] A. L. Efros, M. Rosen, *Annu. Rev. Mater. Sci.* **2000**, *30*, 475 – 521.
[4] A. D. Yoffe, *Adv. Phys.* **2001**, *50*, 1 – 208.
[5] F. V. Mikulec, M. Kuno, M. Bennati, D. A. Hall, R. G. Griffin, M. G. Bawendi, *J. Am. Chem. Soc.* **2000**, *122*, 2532 – 2540.
[6] B. O. Dabbousi, J. Rodriguez-Viejo, F. V. Mikulec, J. R. Heine, H. Mattoussi, R. Ober, K. F. Jensen, M. G. Bawendi, *J. Phys. Chem. B* **1997**, *101*, 9463 – 9475.
[7] S. Empedocles, M. G. Bawendi, *Acc. Chem. Res.* **1999**, *32*, 389 – 396.
[8] M. A. Hines, P. Guyot-Sionnest, *J. Phys. Chem.* **1996**, *100*, 468 – 471.
[9] M. Bruchez Jr., M. Moronne, P. Gin, S. Weiss, A. P. Alivisatos, *Science* **1998**, *281*, 2013 – 2016.
[10] S. A. Blanton, A. Dehestani, P. C. Lin, P. Guyot-Sionnest, *Chem. Phys. Lett.* **1994**, *229*, 317 – 322.
[11] M. Nirmal, B. O. Dabbousi, M. Bawendi, J. J. Macklin, J. K. Trautmann, T. D. Harris, L. E. Brus, *Nature* **1996**, *383*, 802 – 804.
[12] J. Tittel, F. Koberling, T. Basché, A. Kornowski, H. Weller, A. Eychmüller, *J. Phys. Chem. B* **1997**, *101*, 3013 – 3016.
[13] M. Kuno, D. P. Fromm, H. F. Hamann, A. Gallagher, D. J. Nesbitt, *J. Chem. Phys.* **2000**, *112*, 3117 – 3120.
[14] M. Kuno, D. P. Fromm, H. F. Hamann, A. Gallagher, D. J. Nesbitt, *J. Chem. Phys.* **2001**, *115*, 1028 – 1040.
[15] W. C. W. Chan, S. Nie, *Science* **1998**, *281*, 2016 – 2018.
[16] M. Dahan, T. Laurence, F. Pinaud, D. S. Chemla, A. P. Alivisatos, M. Sauer, S. Weiss, *Opt. Lett.* **2001**, *26*, 825 – 827.
[17] D. Gerion, F. Pinaud, S. C. Williams, W. J. Parak, D. Zanchet, S. Weiss, A. P. Alivisatos, *J. Phys. Chem. B* **2001**, *105*, 8861 – 8871.
[18] X. Michalet, F. Pinaud, T. D. Lacoste, M. Dahan, M. P. Bruchez, A. P. Alivisatos, S. Weiss, *Single Mol.* **2001**, *2*, 261 – 276.
[19] A. L. Efros, M. Rosen, *Phys. Rev. Lett.* **1997**, *78*, 1110 – 1113.
[20] U. Banin, M. Bruchez, A. P. Alivisatos, T. Ha, S. Weiss, D. S. Chemla, *J. Chem. Phys.* **1999**, *110*, 1195 – 1201.
[21] M. Y. Shen, M. Oda, T. Goto, *Phys. Rev. Lett.* **1999**, *82*, 3915 – 3918.
[22] T. D. Krauss, L. E. Brus, *Phys. Rev. Lett.* **1999**, *83*, 4840 – 4843.
[23] R. G. Neuhauser, K. T. Shimizu, W. K. Woo, S. A. Empedocles, M. G. Bawendi, *Phys. Rev. Lett.* **2000**, *85*, 3301 – 3304.
[24] A. I. Ekimov, A. L. Efros, T. V. Shubina, A. P. Skvortsov, *J. Lumin.* **1990**, *46*, 97 – 100.
[25] S. A. Empedocles, M. G. Bawendi, *Science* **1997**, *278*, 2114 – 2117.
[26] S. R. Cordero, P. J. Carson, R. A. Estabrook, G. F. Strouse, S. K. Buratto, *J. Phys. Chem. B* **2000**, *104*, 12137 – 12142.
[27] W. G. J. H. M. van Sark, P. L. T. M. Frederix, D. J. van den Heuvel, H. C. Gerritsen, A. A. Bol, J. N. J. van Lingen, C. de Mello Donegá, A. Meijerink, *J. Phys. Chem. B* **2001**, *105*, 8281 – 8284.
[28] F. Koberling, A. Mews, T. Basché, *Adv. Mater.* **2001**, *13*, 672 – 676.
[29] W. M. Yen, S. Shionoya, *Phosphor Handbook,* CRC Press, Boca Raton, FL, **1999**.
[30] W. G. J. H. M. van Sark, P. L. T. M. Frederix, D. J. van den Heuvel, A. A. Bol, J. N. J. van Lingen, C. de Mello Donegá, H. C. Gerritsen, A. Meijerink, *J. Fluoresc.* **2002**, *12*, 69 – 76.

[31] G. Schlegel, J. Bohnenberger, I. Potapova, A. Mews, *Phys. Rev. Lett.* **2002**, *88*, 137 401.
[32] U. Woggon, O. Wind, F. Gindele, E. Tsitsishvili, M. Müller, *J. Lumin.* **1996**, *70*, 269 – 280.
[33] J. R. Lakowicz, I. Gryczynski, G. Piszczek, C. J. Murphy, *J. Phys. Chem. B* **2002**, *106*, 5365 – 5370.
[34] C. Xu, W. W. Webb, *J. Opt. Soc. Am. B* **1996**, *13*, 481 – 491.
[35] M. A. Albota, C. Xu, W. W. Webb, *Appl. Opt.* **1998**, *37*, 7352 – 7356.
[36] X.-Q. Li, Y. Arakawa, *Phys. Rev. B* **1999**, *60*, 1915 – 1920.
[37] P. L. T. M. Frederix, PhD thesis, Utrecht University (The Netherlands) **2001**.
[38] S. A. Blanton, M. A. Hines, P. Guyot-Sionnest, *Appl. Phys. Lett.* **1996**, *69*, 3905 – 3907.
[39] S. A. Empedocles, R. Neuhauser, K. Shimizu, M. G. Bawendi, *Adv. Mater.* **1999**, *11*, 1243 – 1256.
[40] J. E. Bowen Katari, V. L. Colvin, A. P. Alivisatos, *J. Phys. Chem.* **1994**, *98*, 4109 – 4117.
[41] A. Henglein, *Top. Curr. Chem.* **1988**, *143*, 113 – 180.
[42] D. E. Dunstan, A. Hagfeldt, M. Almgren, H. O. G. Siegbahn, E. Mukhtar, *J. Phys. Chem.* **1990**, *94*, 6797 – 6804.
[43] L. Spanhel, M. Haase, H. Weller, A. Henglein, *J. Am. Chem. Soc.* **1987**, *109*, 5649 – 5655.
[44] A. L. Rogach, L. Katsikas, A. Kornowski, D. Su, A. Eychmüller, H. Weller, *Ber. Bunsen-Ges* **1997**, *101*, 1668 – 1670.
[45] T. D. Krauss, L. E. Brus, *Mater. Sci. Eng. B* **2000**, *69 – 70*, 289 – 294.
[46] S. M. Sze, *Physics of Semiconductor Devices, 2nd ed.*, Wiley, New York, NY, **1981**.
[47] M. Ohring, *The Materials Science of Thin Films,* Academic Press, San Diego, CA, **1992**.
[48] K. T. Shimizu, R. G. Neuhauser, C. A. Leatherdale, S. A. Empedocles, W. K. Woo, M. G. Bawendi, *Phys. Rev. B* **2001**, *63*, 205 316.
[49] I. Rosenthal, *Opt. Commun.* **1978**, *24*, 164 – 166.
[50] A. L. Huston, C. T. Reimann, *Chem. Phys.* **1991**, *149*, 401 – 407.
[51] Th. Schmidt, G. J. Schütz, W. Baumgartner, H. J. Gruber, H. Schindler, *Proc. Natl. Acad. Sci. USA* **1996**, *93*, 2926 – 2929.
[52] G. Messin, J. P. Hermier, E. Giacobino, P. Desbiolles, M. Dahan, *Opt. Lett.* **2001**, *26*, 1891 – 1893.
[53] N. Chestnoy, T. D. Harris, R. Hull, L. E. Brus, *J. Phys. Chem.* **1986**, *90*, 3393 – 3399.
[54] L. Song, C. A. G. O. Varma, J. W. Verhoeven, H. J. Tanke, *Biophys. J.* **1996**, *70*, 2959 – 2968.
[55] V. Ladizhansky, G. Hodes, S. Vega, *J. Phys. Chem. B* **2000**, *104*, 1939 – 1943.
[56] A. A. Bol, PhD thesis, Utrecht University (The Netherlands) **2001**.
[57] R. P. Haugland, *Handbook of Fluorescent Probes and Research Chemicals*, Molecular Probes, Eugene, OR, **2001**.
[58] P. L. T. M. Frederix, M. A. H. Asselbergs, W. G. J. H. M. van Sark, D. J. van - den Heuvel, W. Hamelink, E. L. De Beer, H. C. Gerritsen, *Appl. Spectrosc.* **2001**, *55*, 1005 – 1012.
[59] J. Sytsma, J. M. Vroom, C. J. De Grauw, H. C. Gerritsen, *J. Microsc. (Oxford, UK)* **1998**, *191*, 39 – 51.
[60] C. J. De Grauw, J. M. Vroom, H. T. M. Van der Voort, H. C. Gerritsen, *Appl. Opt.* **1999**, *38*, 5995 – 6003.
[61] C. J. De Grauw, H. C. Gerritsen, *Appl. Spec.* **2001**, *55*, 670 – 678.

Received: April 30, 2002 [F 410]